Dalton Transactions

PAPER

View Article Online
View Journal

Check for updates

Cite this: DOI: 10.1039/c7dt02752d

A series of sulfonic acid functionalized mixed-linker DUT-4 analogues: synthesis, gas sorption properties and catalytic performance†

Guang-Bo Wang,[a] Karen Leus,[a] Kevin Hendrickx,[a,b] Jelle Wieme,[b] Hannes Depauw,[a] Ying-Ya Liu,[c] Veronique Van Speybroeck[b] and Pascal Van Der Voort*[a]

In this work, we present the successful synthesis of a series of sulfonic acid functionalized mixed-linker metal–organic frameworks (MOFs) having the DUT-4 topology by using different ratios of 2,6-naphthalenedicarboxylic acid (H_2-NDC) and 4,8-disulfonaphthalene-2,6-dicarboxylic acid (H_2-NDC-2SO_3H) in one-pot reactions. The obtained materials were fully characterized and their CO_2 adsorption properties at low and high pressures were studied and compared with those of the pristine DUT-4 material. Generally, the CO_2 adsorption capacities range from 3.28 and 1.36 mmol g^{-1} for DUT-4 to 1.54 and 0.78 mmol g^{-1} for DUT-4-SO_3H (50) up to 1 bar at 273 K and 303 K, respectively. Computational calculations corroborated the structural changes of the material in function of the loading of sulfonic acid groups. Furthermore, due to the strong Brønsted acid character, the resulting sulfonic acid based MOF material was evaluated as a catalyst for the ring opening of styrene oxide with methanol as a nucleophile under mild conditions, showing almost full conversion (99%) after 5 hours of reaction. A hot filtration experiment demonstrated that the catalysis occurred heterogeneously and the catalyst could be recovered and reused for multiple runs without significant loss in activity and crystallinity.

Received 28th July 2017,
Accepted 26th September 2017

DOI: 10.1039/c7dt02752d

rsc.li/dalton

Published on 13 October 2017. Downloaded by Freie Universitaet Berlin on 13/10/2017 09:25:05.

Introduction

Metal organic frameworks (MOFs), also known as porous coordination polymers (PCPs), are hybrid materials widely examined in various applications ranging from gas sorption and separation[1–4] to heterogeneous catalysis.[5–8] They owe this large interest to their unique structural tailorability, good crystallinity and controlled surface area and porosity.[9] Moreover, the concept of isoreticular synthesis allows one to introduce specific functionalities into the framework whilst retaining the topology of a given framework structure.[10,11] To date, tremendous efforts and strategies have been reported to embed multiple functional groups into given MOFs. Amongst them, the mixed-linker approach, where different linkers are mixed before synthesis, has been examined extensively in recent years since it preserves the structural integrity and is a very straightforward procedure.[12–15] Baiker and co-workers have used this mixed-linker approach to synthesize a series of amine functionalized MOF-5 materials with the general formula $[Zn_4O(BDC)_x(BDC\text{-}NH_2)_{3-x}]$ in which x can be varied and the obtained materials were tested as catalysts in the reaction of propylene oxide and CO_2 forming propylene carbonate.[5] Yaghi and co-workers successfully synthesized a series of multivariate (MTV) MOFs by incorporating eight different functionalities into MOF-5 under solvothermal conditions, in which the amount of the introduced functional groups could be varied.[1] In the work of Cohen *et al.*[16] and Bordiga *et al.*,[14] the synthesis and characterization of amine functionalized mixed-linker metal–organic frameworks having a UiO-66 topology was described. Another class of materials that has received considerable attention in the field of isoreticular synthesis is the MIL-53 type of material due to its interesting structural flexibility upon external stimuli (*e.g.* guest molecule adsorption/desorption).[3,17–19]

The incorporation of sulfonic acid functional groups into MOFs has a significant impact on the gas sorption properties and in potential catalytic and proton conduction applications.[20,21] Within this context, Zhou and co-workers reported

[a]Department of Inorganic and Physical Chemistry, Center for Ordered Materials, Organometallics and Catalysis (COMOC), Ghent University, Krijgslaan 281 (S3), 9000 Ghent, Belgium. E-mail: pascal.vandervoort@ugent.be
[b]Center for Molecular Modeling, Ghent University, Technologiepark 903, 9052 Zwijnaarde, Belgium
[c]State Key Laboratory of Fine Chemicals, Dalian University of Technology, 116024 Dalian, People's Republic of China

†Electronic supplementary information (ESI) available. See DOI: 10.1039/c7dt02752d

Published on 13 October 2017. Downloaded by Freie Universitaet Berlin on 13/10/2017 09:25:05.

on the introduction of sulfonic acid functional groups into a porous polymer network (PPN-6-SO_3H), which significantly increased the CO_2 adsorption capacity and CO_2/N_2 selectivity.[22] Stock *et al.* synthesized a series of sulfo-functionalized mixed-linker CAU-10 analogues, in which the polar groups significantly influence the sorption capacities towards N_2, H_2 and CO_2.[23] By using the mixed-linker approach, a series of sulfonic acid functionalized mixed-linker UiO-66 materials was successfully synthesized by the group of Kitagawa, after which an enhanced CO_2 adsorption capacity and isosteric heat of CO_2 adsorption was noted.[24] Moreover, the presence of sulfonic acid groups can be beneficial for various catalytic reactions.[25] The acid catalyzed ring opening of epoxides with various nucleophiles can provide an easy access to various intermediates, which are widely desired in the pharmaceutical industry.[26] Pioneering work on the use of MOFs in these reactions was done by Baiker *et al.*, who examined a copper based MOF under ambient and solvent-free conditions.[27] Later on, some commercially available MOFs were systematically studied by Garcia and co-workers.[28,29] Recently, a ~100% sulfonic acid functionalized MIL-101 material (MIL-101-SO_3H) was synthesized exhibiting an exceptionally high efficiency and recyclability in the ring opening reaction of styrene oxide.[30] In another recent report of Farha and co-workers, seven Zr/Hf-based UiO-type MOFs with different degrees of defects were studied for their catalytic activity in the epoxide ring-opening reaction, which proved that the catalytic activity improved with increasing the numbers of defects in the MOFs.[31]

In this contribution, we report the synthesis and characterization of a series of sulfonic acid functionalized mixed-linker DUT-4 analogues by using various ratios of the linker 2,6-naphthalenedicarboxylic acid (H_2-NDC) and 4,8-disulfonaphthalene-2,6-dicarboxylic acid (H_2-NDC-2SO_3H) in one-pot reactions. The CO_2 and N_2 gas sorption properties of all the obtained compounds were evaluated and compared with those of the pristine DUT-4 material. Additionally, a selected material, named DUT-4-SO_3H(30), was examined for its catalytic performance in the ring opening of styrene oxide under mild reaction conditions.

Experimental section

Chemicals

The organic ligand H_2-NDC-2SO_3H was synthesized according to a previously reported procedure.[32] All other chemicals were purchased from Sigma Aldrich or TCI Europe and used without further purification.

Synthesis of $Al(OH)(NDC)_{1-x}(NDC\text{-}2SO_3H)_x$

The detailed ratios and employed amounts of starting materials for the synthesis of the mixed-linker MOF series are listed in Table S1, ESI.† Typically, 0.26 g (0.69 mmol) $Al(NO_3)_3{\cdot}9H_2O$ and a specific ratio of H_2-NDC and H_2-NDC-2SO_3H were dissolved in 15 mL *N*,*N*-dimethylformamide (DMF). The resulting mixture was stirred for 5 minutes at room temperature, sealed in a 23 mL Teflon-lined stainless steel vessel and heated to 150 °C for 24 hours. After cooling down to room temperature, the obtained solid was collected by membrane filtration and thoroughly washed with DMF, methanol and acetone. Thereafter, the material was dried under vacuum at room temperature prior to analysis. The obtained materials were denoted as DUT-4-$SO_3H(x)$, in which x corresponds to the theoretical percentage of H_2-NDC-2SO_3H used during the synthesis.

Experimental and analytical techniques

X-ray powder diffraction (XRPD) patterns were collected on a Thermo Scientific ARL X'Tra diffractometer, operated at 40 kV, 30 mA using Cu-K_α radiation (λ = 1.5406 Å). Peak indexing and refinement of the unit cell parameters were performed with the TOPAS suite using the Pawley method.[33] Peaks were fitted with a TCHZ pseudo-Voigt profile and a simple axial model to correct for peak asymmetry. Fourier transform infrared spectroscopy (FT-IR) in the region of 400–4000 cm^{-1} was performed with a Thermo Nicolet 6700 FT-IR spectrometer equipped with a nitrogen-cooled Mercury Cadmium Telluride (MCT) detector and a KBr beam splitter. Thermogravimetric analysis (TGA) was done on a Netzsch STA-449 F3 Jupiter-simultaneous TG-DSC analyzer in the temperature range of 20–800 °C in air at a heating rate of 2 °C min^{-1}. ^1H NMR spectra of all the obtained MOFs, digested in a mixture of D_2SO_4/DMSO-d_6, were recorded on a Bruker 300 MHz Avance spectrometer. The reaction products were identified with a TRACE GC × GC (Thermo, Interscience), coupled to a TEMPUS TOF-MS detector (Thermo, Interscience). The first column consists of a dimethyl polysiloxane package and has a length of 50 m, with an internal diameter of 0.25 mm, whereas the second column has a length of 2 m with an internal diameter of 0.15 mm. The package of the latter is a 50% phenyl polysilphenylene-siloxane and helium was used as a carrier gas. Inductively coupled plasma-optical emission spectroscopy (ICP-OES) measurements were performed to determine the sulfur leaching using a Varian 715-ES. Scanning electron microscopy (SEM) images of the catalyst before and after catalysis were recorded on a JEOL JSM-7600F FEG-SEM. N_2 adsorption isotherms were obtained using Belsorp Mini apparatus measured at 77 K, whereas CO_2 adsorption measurements were carried out on a Quantachrome iSorb-HP gas sorption analyzer. Prior to the gas sorption measurements, all the materials were activated at a heating rate of 2 °C min^{-1} up to 150 °C under vacuum for 3 h.

Catalytic setup

In a typical catalytic test, a 25 mL Schlenk flask was loaded with 10 mL of methanol and 2 mmol of dodecane used as a solvent and internal standard, respectively, 2 mmol styrene oxide and a loading (based on sulfonic acid groups) of 5 mol% of DUT-4-SO_3H(30) was employed. All the catalytic tests were performed in air while stirring at 55 °C. The reaction was monitored periodically by GC until full conversion was obtained. Afterwards, the catalyst was recovered by means of centrifugation and the filtrate was analyzed by ICP-OES to

 This journal is © The Royal Society of Chemistry 2017

Published on 13 October 2017. Downloaded by Freie Universitaet Berlin on 13/10/2017 09:25:05.

examine the sulfur leaching. The recovered catalyst was activated at 150 °C under vacuum and reused in multiple runs.

Computational details

Two types of calculations were performed to obtain more insight into the structural changes of the materials upon loading with sulfonic acid groups and the corresponding catalytic activity. First of all, periodic Density Functional Theory (DFT) calculations were performed with the Vienna *Ab Initio* Simulation Package (VASP)[34] using the projector-augmented wave (PAW) method on three materials with various loadings of sulfonic acid groups (see Fig. 4).[35] The ionic positions and lattice cell parameters were relaxed at the experimental volume of the material. The PBE functional[36] is used together with D3 empirical dispersion corrections with Becke–Johnson damping.[37,38] An energy cutoff of 500 eV is used together with a 2 × 6 × 2 *k*-point mesh similar to the work of Vanpoucke *et al.*[39] A Gaussian smearing scheme with σ equal to 0.05 eV is employed. An electronic convergence criterion of 10^{-6} eV is used together with an ionic convergence of 10^{-4} eV. The textural properties such as pore diameter and accessible surface area are calculated with Zeo++ with a probe with diameter of 3.64 Å, resembling the kinetic diameter of N_2.[40]

To obtain more insight into the size of the reactant molecules (styrene oxide and 2-methoxy-2-phenylethanol) for catalysis and their fitting into the various materials, molecular calculations were done within the Gaussian09 program using a B3LYP hybrid functional[41,42] and a Pople 6-311+G(d,p) basis set.[43] Furthermore, solvent effects were included using a polarizable continuum model (with ε = 32.613)[44] to mimic the methanol solvation of the reactants during a catalytic run.

Results and discussion

Synthesis and characterization of the DUT-4-SO_3H(x) materials

The synthesis of the sulfonic acid functionalized mixed-linker DUT-4 analogues was performed in a one-pot reaction by varying the initial ratio of H_2-NDC and H_2-NDC-2SO_3H linkers (Scheme 1), applying similar reaction conditions as reported for the synthesis of the pristine DUT-4 material.[45] Table S1† shows that at a reaction temperature of 150 °C for 24 hours, up to 50% of the H_2-NDC-2SO_3H linker can be introduced into the DUT-4 framework. To confirm the framework topology of the obtained materials, XRPD measurements were performed (Fig. 1 and Fig. S1†). The mixed-linker MOFs are crystalline and isostructural, having the same topology as the pristine DUT-4 framework. It should be noted that a significant decrease in the crystallinity is observed as the ratio of H_2-NDC-2SO_3H is higher than 50% and a considerable amount of amorphous phase was obtained at a substitution of 100% of H_2-NDC-2SO_3H, showing that it is not possible to synthesize the pure sulfonic acid functionalized DUT-4 material under the examined reaction conditions. A simple Pawley refinement of the experimental diffractogram allowed us to refine the unit cell parameters, starting from the literature values for the pristine DUT-4 (*a*: 18.825 Å; *b*: 6.787 Å; *c*: 16.901 Å) and using the same orthorhombic space group *Pnna*.[45] After refinement, slightly smaller values of the unit cell dimensions were found (*a*: 18.26 Å; *b*: 6.73 Å; *c*: 16.64 Å) yielding a unit cell volume of 2064 Å^3. The weighted profile *R*-factor (R_{wp}) was 15.15 after refinement and a χ^2 of 1.78 was obtained. Additionally, the successful incorporation of the functionalized linker molecules into the DUT-4 structure was confirmed by FT-IR measurements (Fig. S2†). The bands at 1205 cm^{-1} and 1145 cm^{-1} are attributed to the O═S═O stretching vibrations whereas the vibration at 1038 cm^{-1} can be assigned to the S–O stretching vibration.[46,47] The absence of the band at ~1680 cm^{-1} confirms that there is no residual free carboxylate linker in the structure. The actual composition of the mixed linkers in the resulting MOFs was determined *via* ^{1}H NMR spectroscopy by digesting the obtained mixed-linker MOFs into a mixture of D_2SO_4–DMSO-d_6. The obtained ^{1}H NMR spectra are shown in Fig. 2, while ratios calculated *via* integrating their respective proton peaks are listed in Table S1.† By increasing the ratio of the H_2-NDC-2SO_3H linker (from 0 to 50%) used in the initial reaction mixture, a progressive increase of the ^{1}H NMR signals associated with the H_2-NDC-2SO_3H linker is observed. Notably, in all cases, the quantity of the H_2-NDC-2SO_3H linkers observed in the resulting

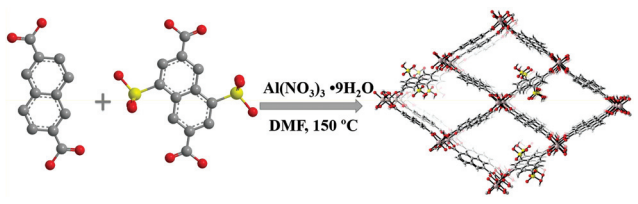

Scheme 1 Schematic representation of the synthesis of the mixed-linker metal–organic frameworks possessing the DUT-4 topology, which is denoted as DUT-4-SO_3H(x).

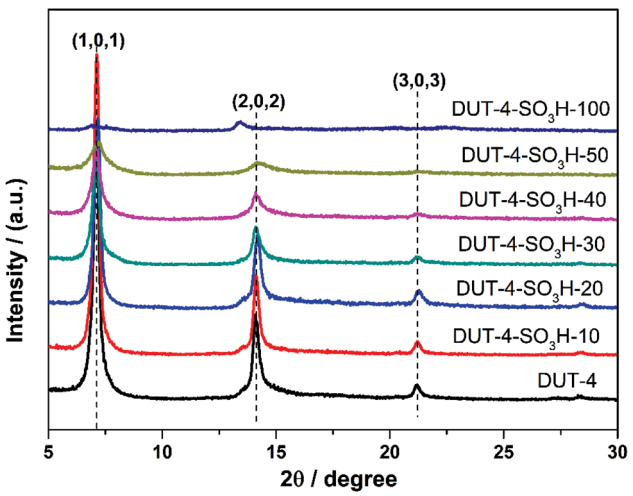

Fig. 1 XRPD patterns of the sulfonic acid functionalized mixed-linker DUT-4-SO_3H(x) materials, x = 0, 10, 20, 30, 40, 50, and 100.

Published on 13 October 2017. Downloaded by Freie Universitaet Berlin on 13/10/2017 09:25:05.

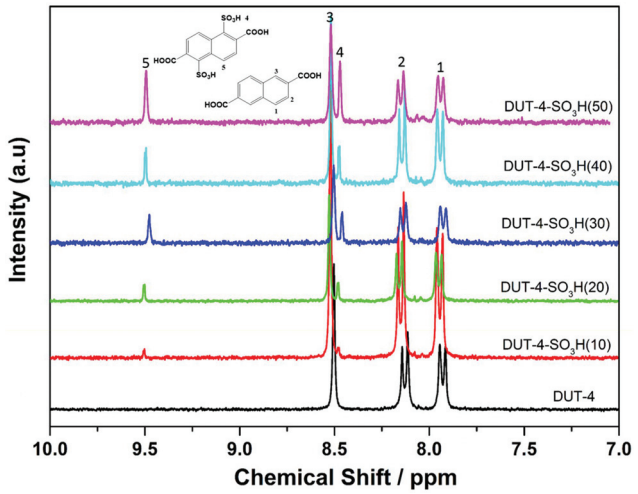

Fig. 2 ^{1}H NMR spectra of the digested mixed-linker DUT-4 analogues.

MOFs is somewhat less than the amount that was added initially to the reaction mixture, demonstrating that the non-functionalized organic linker is preferentially incorporated.

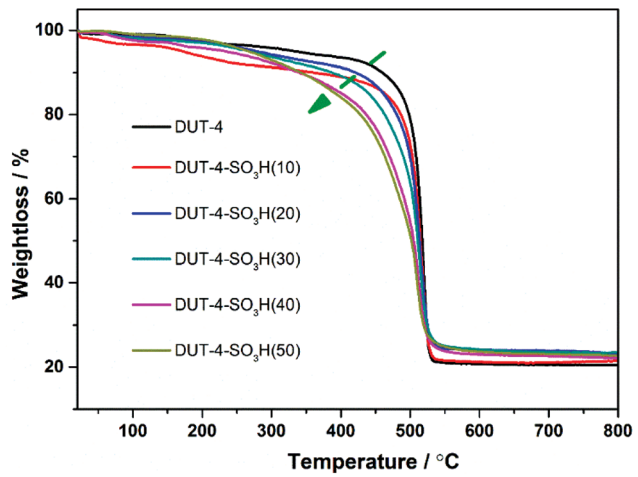

Fig. 3 TGA curves of the mixed-linker DUT-4 analogues measured under an air flow at a heating rate of 2 °C min^{-1}.

This observation is consistent with previously published reports on functionalized MOF-5 and sulfonic acid functionalized mixed-linker UiO-66 type of material.[1,24] TGA was used to determine the thermal stability of the resulting mixed-linker MOF materials and the thermogravimetric curves are depicted in Fig. 3. From this figure, the thermal stability of the functionalized materials gradually decreases with increasing amount of H_2-NDC-2SO_3H. The pristine DUT-4 material has a decomposition temperature of 450 °C, while the DUT-4-SO_3H (50) starts to decompose at 300 °C. A similar trend in stability has also been observed for a series of mixed-linker MOFs having the MIL-53 [17] and IRMOF-3/MOF-5 topology.[48]

In order to gain more insight into the structural changes induced by the functional groups, structural relaxations on 3 different materials were performed. We studied the pristine material of DUT-4 and two materials with different loadings of sulfonic acids namely, DUT-4-SO_3H(25) and DUT-4-SO_3H(100), corresponding to a substitution pattern of 25 and 100%. For the 25% functionalized material, the SO_3H groups were placed along a chain parallel to the *b*-axis. Fig. 4 shows that a torsion of the functionalized linkers occurs, and hence the SO_3H group points inside the pore, which is beneficial for its accessibility during catalysis. However, this also induces a contraction of the pore along the *c*-axis, which becomes even more pronounced when looking at the 100% loaded material. Here, the SO_3H groups can interact *via* hydrogen bonds, blocking the entire pore system of the material. This strong interaction also gives a hint why the materials with a high SO_3H loading form less crystalline or even amorphous materials. We think that the strongly interacting sulfonic groups could interfere during the synthesis and hinder the crystallization process. Moreover, interaction between the groups within the framework could lead to increased strain and lower the crystallinity of the material in that way. Table S3† depicts the calculated internal diameters of the three materials, showing a gradual decrease of this parameter.

Gas sorption properties

The porosity of the resulting mixed-linker MOFs was determined by means of N_2 adsorption. As shown in Fig. 5, all the resulting materials exhibit a typical type I isotherm, which is characteristic of microporous materials. As expected, the

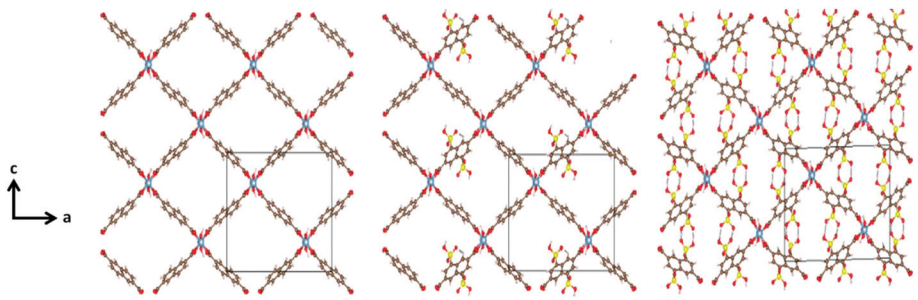

Fig. 4 Representation of the 3 materials considered in the computational study. DUT-4 (left), DUT-4-SO_3H(25) (middle) and DUT-4-SO_3H(100) (right).

This journal is © The Royal Society of Chemistry 2017

Published on 13 October 2017. Downloaded by Freie Universitaet Berlin on 13/10/2017 09:25:05.

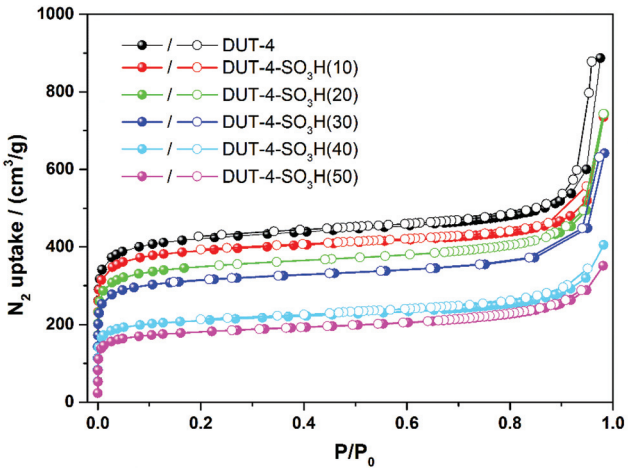

Fig. 5 N_2 adsorption (solid symbols) and desorption (open symbols) isotherms of the resulting mixed-linker DUT-4-$SO_3H(x)$ materials.

Langmuir surface area and pore volume of the obtained materials gradually decreases with increasing the amount of sulfonic acid functionalized linker. This could be attributed to the presence of the extra functional groups as well as a contraction of the pores, reducing the total available pore volume. The Langmuir and BET surface areas and pore volume of 1950 $m^2\ g^{-1}$, 1650 $m^2\ g^{-1}$ and 0.63 $cm^3\ g^{-1}$, respectively, are obtained for DUT-4, while the Langmuir and BET surface areas of 820 $m^2\ g^{-1}$ and 546 $m^2\ g^{-1}$ and pore volume of 0.23 $cm^3\ g^{-1}$ are obtained for DUT-4-$SO_3H(50)$. The detailed Langmuir and BET surface areas and pore volumes of all the mixed-linker MOFs are summarized in Table S1.†

Furthermore, to investigate the influence of the sulfonic acid functional groups on the gas sorption properties, low pressure CO_2 adsorption isotherms for all the activated samples were recorded up to 1 bar at 273 and 303 K (see Fig. 6). From this figure one can see that the CO_2 adsorption capacity of all the samples increases linearly with the pressure, without reaching a saturation in the studied pressure region. The CO_2 adsorption capacity ranges from 3.28 and 1.36 mmol g^{-1} for DUT-4 to 1.54 and 0.78 mmol g^{-1} for DUT-4-$SO_3H(50)$ at 273 and 303 K, respectively. It should be noted that the incorporation of sulfonic acid groups does not increase the CO_2 adsorption capacity of the studied materials, which mainly follows the trend of the available pore volume of the compounds. This behavior has been previously observed and reported by Stock *et al.*[23] Additionally, to provide a better understanding of the CO_2 adsorption properties, the isosteric heats (Q_{st}) of CO_2 adsorption were calculated from the CO_2 adsorption isotherms measured at different temperatures using the Clausius–Clapeyron equation (see ESI†).[49] As expected, the trend of the Q_{st} for the series of MOFs is the same as the CO_2 adsorption capacity discussed above, decreasing from 20.4 kJ mol^{-1} for DUT-4 to 14.3 kJ mol^{-1} for DUT-4-$SO_3H(50)$ (Fig. S3†). High-pressure CO_2 adsorption isotherms were also recorded at 273 and 303 K and are shown in Fig. S4.† At both temperatures, the obtained isotherms show a type I profile with final CO_2 adsorption capacities ranging from 13.7 and 10.7 mmol g^{-1} for DUT-4 to 6.3 and 5.4 mmol g^{-1} for DUT-4-$SO_3H(50)$ at 273 and 303 K, respectively, and a pressure of up to 20 bar. Notably, the saturation capacity significantly decreases as the loading of sulfonic acid groups reaches 50%, which is mainly due to the severely reduced pore volume and surface area of the materials.

Catalytic performance of DUT-4-$SO_3H(30)$

The presence of strong Brønsted acid sites within the obtained DUT-4-$SO_3H(x)$ materials allows us to examine them as a catalyst in the ring opening of styrene oxide under mild conditions (Fig. 7a). Based on the structural study, the DUT-4-$SO_3H(30)$ was chosen as a catalyst due to its good crystallinity, high surface area and pore volume as well as the desirable content of sulfonic acid groups. Furthermore, we showed *via* structural optimizations on the pristine and functionalized materials that upon increasing the amount of functional groups in the unit cell, the internal diameter of the material decreases (Table S3†). If we compare this diameter with the size of the reactant molecules (styrene oxide), they are in the same order of magnitude (Fig. S5†). The pristine DUT-4 has a larger internal diameter than the reactant size, however, the 25% loaded material of the computational study already has a slightly smaller pore opening than the long axis of the reac-

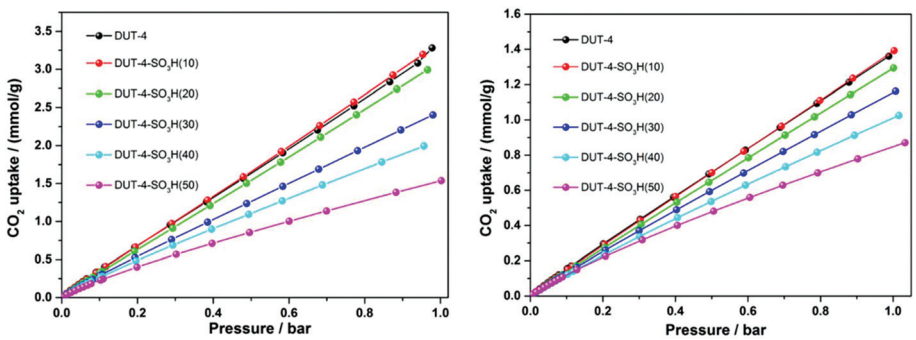

Fig. 6 CO_2 adsorption isotherms (up to 1 bar) of the mixed linker DUT-4-$SO_3H(x)$ materials measured at 273 K (left) and 303 K (right), respectively.

Published on 13 October 2017. Downloaded by Freie Universitaet Berlin on 13/10/2017 09:25:05.

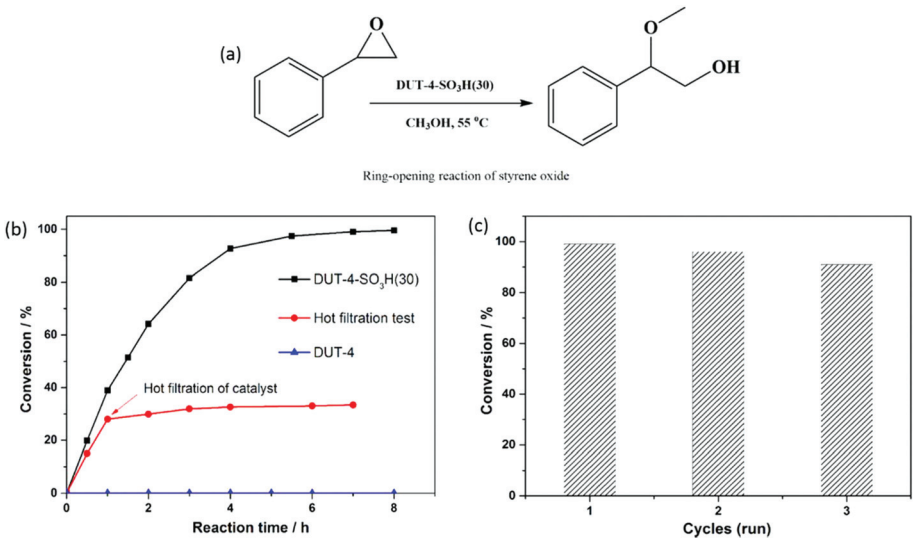

Fig. 7 (a) Styrene oxide ring-opening reaction with methanol, catalyzed by MOFs; (b) time–conversion plot for the ring opening reaction of styrene oxide using DUT-4 and DUT-4-SO_3H(30) as a catalyst and the performed hot filtration test; and (c) reusability of the catalyst in 3 successive runs for the ring opening of styrene oxide with methanol.

tant, thus, the epoxide can only diffuse into the material in one way, which limits the rate of the reaction. For the 100% SO_3H loaded material, the pores contract even further and the reactants are now completely inhibited to enter the material or in other words the SO_3H groups which are located on the outer surface of the material would be only accessible. The loading of 25–30% is therefore an optimal trade-off between the presence of sufficient functional groups and still enough opening of the pores to allow for diffusion of the reactant molecules used in this study. For comparison, we also examined the catalytic activity of the DUT-4 material. Fig. 7b shows that the DUT-4 material gave a negligible conversion after 8 h of reaction. This is due to the fact that the Al^{3+} ions in DUT-4 are fully saturated by NDC linkers and therefore no free metal sites are available as Lewis acids to promote the reaction. For the DUT-4-SO_3H(30), almost full conversion was observed after 5 h of reaction. To verify whether the reaction is completely heterogeneous, a hot filtration test was done in which the mixture was filtered off after 1 h of reaction (Fig. 7b). After the removal of the catalyst, no further conversion of styrene oxide was observed in the filtrate, demonstrating that the catalysis is heterogeneous. ICP analysis of the filtrate showed a negligible amount of sulfur leaching (~0.4%) after the first run. In Table 1, a comparison is made with some other literature reported MOF materials that have been used for the ring opening of styrene oxide. The active acid sites of the examined MOFs are either Lewis or Brønsted acids and most of them can achieve full conversion within a reasonable time except for the HP-CuBTC-0.25 for which only a conversion of 35.6% was obtained after 4 h of reaction. Although it is difficult to make a fair comparison as different reaction conditions were used, the MIL-101-SO_3H seems to be the best catalyst and has a relatively

Table 1 Comparison of the catalytic performance of DUT-4-SO_3H(30) with other reported MOF catalysts used for the ring opening of styrene oxide

Entry	Catalyst	T (min)	T (°C)	Conv. (%)	TON/TOF (h^{-1})	Ref.
1	Cu-MOF	3 h	RT	99	—/5.3	27
2	Fe(BTC)	60	40	>99	—/10	29
3	HKUST-1	2.5 h	40	90	—	50
4	HKUST-1/ATP	20	50	98.9	—/3.32–4.44	51
5	MIL-101-SO_3H	30	RT	>99	—/99	30
6	MIL-101(HPW)	20	40	99 (dropped to 62 in the 3rd run)	—	52
7	HP-CuBTC-0.25	4 h	40	35.6	—	53
8	Zr-UiO-66	24 h	55	40[a]	—	31
9	Zr-MOF-808	24 h	55	100[a]	—	31
10	UiO-66-X (X = H, NH_2, NO_2, Br, Cl)	24 h	50	96[b]	—	28
11	DUT-4-SO_3H(30)	6 h	55	>99	20[c]/8[d]	This work

[a] Isopropanol as the nucleophile. [b] The conversion is based on the catalyst of UiO-66-Br. [c] The TON value was calculated after 5 h of catalysis. [d] The TOF value was calculated after 0.5 h of catalysis.

This journal is © The Royal Society of Chemistry 2017

Published on 13 October 2017. Downloaded by Freie Universitaet Berlin on 13/10/2017 09:25:05.

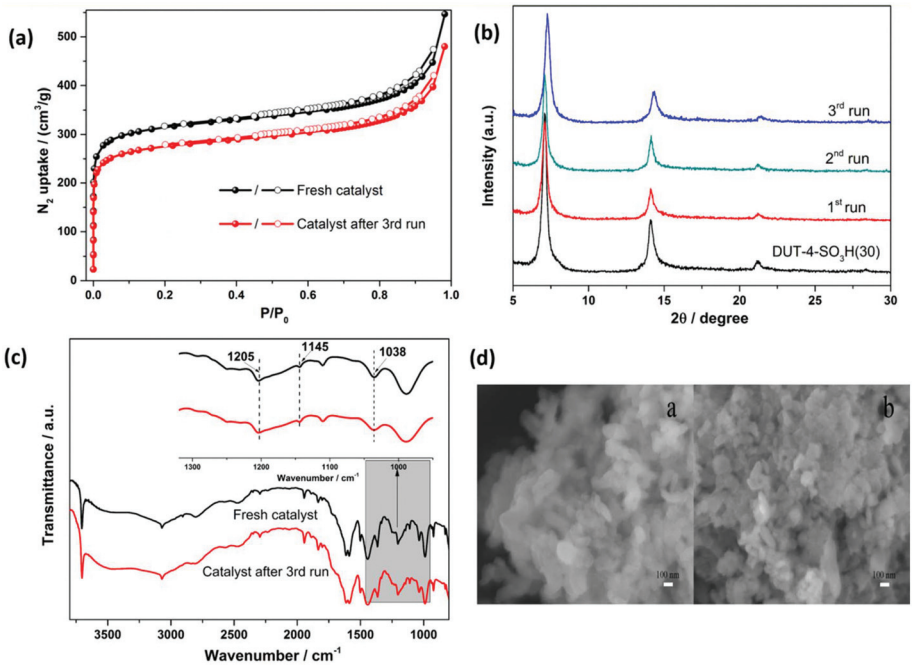

Fig. 8 (a) XRPD patterns of the catalyst before and after each run; (b) N_2 sorption isotherms of the catalyst before and after the 3rd run; (c) FT-IR spectra of the fresh catalyst (black) and the catalyst after the 3rd run (red). Inset: Details on the region of 900–1350 cm^{-1}. (d) SEM images of the fresh catalyst (a) and the catalyst after the 3rd run (b).

fast reaction rate and a high TOF of 99 h^{-1}. This is probably due to the fact that the compound has mesopores and higher pore volumes in comparison with other reported MOF materials, which will allow a better diffusion and mass transfer.

Additionally, the stability and reusability of the catalyst was examined. After obtaining full conversion, the catalyst was recovered by membrane filtration, washed with acetone (10 mL × 3) and activated at 150 °C under vacuum before it was used in additional runs. As shown in Fig. 7c, only a slight decrease in the catalytic activity is observed after 3 runs. This somewhat lower catalytic activity in the additional runs is probably due to a partial loss of the catalyst during the catalyst recovery and also because of a partial clogging of the pores after the first run, which was confirmed by N_2 adsorption analysis. A slight decrease in the Langmuir surface area was noted in the reused catalyst in comparison with the fresh DUT-4-SO_3H(30) catalyst (see Fig. 8a). Moreover, in the additional runs, no leaching of sulfur was observed demonstrating once more the heterogeneous character of the catalysis. The stability of the catalyst after multiple runs was confirmed by XRPD measurements, which is shown in Fig. 8b. The crystallinity of the recovered catalyst after each catalytic test is well preserved, which demonstrates the good stability of the selected catalyst under the applied reaction conditions. Aside from the XRPD measurements, FT-IR spectra (Fig. 8c) and SEM images (Fig. 8d) of the fresh catalyst and after the third run were collected revealing no significant changes in the morphology of the catalyst.

Conclusion

In conclusion, a series of sulfonic acid functionalized mixed-linker metal–organic frameworks (MOFs) possessing the DUT-4 topology have been successfully synthesized using well-defined ratios of H_2-NDC and H_2-NDC-2SO_3H. The resulting materials were thoroughly characterized by means of XRPD, TGA, FT-IR spectroscopy, SEM, ^{1}H NMR spectroscopy and N_2 sorption. The changes in the pore and textural properties of the materials were studied in detail *via* computational calculations and provided a structural explanation for the observed experimental trends. The effect of the functional groups on the gas sorption properties was examined by CO_2 adsorption measurements. Generally, the CO_2 adsorption capacities range from 3.28 and 1.36 mmol g^{-1} for DUT-4 to 1.54 and 0.78 mmol g^{-1} for DUT-4-SO3H (50) up to 1 bar at 273 K and 303 K, respectively. Furthermore, due to the strong acidic character of the sulfonic acid groups, the DUT-4-SO_3H(30) material was evaluated as a catalyst for the ring opening of styrene oxide under mild conditions reaching full conversion (99%) after 5 h of reaction. Moreover, the DUT-4-SO_3H (30) catalyst could be recovered and reused for three additional cycles without significant loss in activity and stability.

Conflicts of interest

There are no conflicts to declare.

Published on 13 October 2017. Downloaded by Freie Universitaet Berlin on 13/10/2017 09:25:05.

Acknowledgements

The authors are grateful for financial support received from the Research Board of Ghent University (BOF) and BELSPO in the frame of IAP/7/05. G.-B. Wang gratefully acknowledges the Chinese Scholarship Council (CSC) for financial support. K. L. acknowledges financial support from the Ghent University. J. W. acknowledges the Research Foundation Flanders (FWO-Vlaanderen) for financial support. H. D. acknowledges the Research Foundation Flanders (FWO-Vlaanderen) Grant (No. G.0048.13N.). Y.-Y. L. is grateful for financial support from the National Natural Science Foundation of China (No. 21403025) and the Scientific Research Foundation for Returned Scholars, Ministry of Education of China. The computational resources and services used in this work were provided by the VSC (Flemish Supercomputer Center), funded by the Research Foundation Flanders (FWO) and the Flemish Government – department EWI. The authors thank Jeffrey Paulo Perez and Sander Clerick for ICP-OES and SEM measurements respectively.

References

1 H. Deng, C. J. Doonan, H. Furukawa, R. B. Ferreira, J. Towne, C. B. Knobler, B. Wang and O. M. Yaghi, *Science*, 2010, **327**, 846–850.
2 S. H. Jhung, N. A. Khan and Z. Hasan, *CrystEngComm*, 2012, **14**, 7099–7109.
3 T. Lescouet, E. Kockrick, G. Bergeret, M. Pera-Titus, S. Aguado and D. Farrusseng, *J. Mater. Chem.*, 2012, **22**, 10287–10293.
4 G. Wang, K. Leus, S. Couck, P. Tack, H. Depauw, Y.-Y. Liu, L. Vincze, J. F. M. Denayer and P. Van Der Voort, *Dalton Trans.*, 2016, **45**, 9485–9491.
5 W. Kleist, F. Jutz, M. Maciejewski and A. Baiker, *Eur. J. Inorg. Chem.*, 2009, **2009**, 3552–3561.
6 A. M. Rasero-Almansa, A. Corma, M. Iglesias and F. Sánchez, *ChemCatChem*, 2014, **6**, 3426–3433.
7 B. Li, K. Leng, Y. Zhang, J. J. Dynes, J. Wang, Y. Hu, D. Ma, Z. Shi, L. Zhu, D. Zhang, Y. Sun, M. Chrzanowski and S. Ma, *J. Am. Chem. Soc.*, 2015, **137**, 4243–4248.
8 X. Xu, J. A. van Bokhoven and M. Ranocchiari, *ChemCatChem*, 2014, **6**, 1887–1891.
9 H. C. Zhou, J. R. Long and O. M. Yaghi, *Chem. Rev.*, 2012, **112**, 673–674.
10 O. M. Yaghi, M. O'Keeffe, N. W. Ockwig, H. K. Chae, M. Eddaoudi and J. Kim, *Nature*, 2003, **423**, 705–714.
11 M. Eddaoudi, J. Kim, N. Rosi, D. Vodak, J. Wachter, M. O'Keeffe and O. M. Yaghi, *Science*, 2002, **295**, 469–472.
12 Z. Yin, Y.-L. Zhou, M.-H. Zeng and M. Kurmoo, *Dalton Trans.*, 2015, **44**, 5258–5275.
13 A. Dhakshinamoorthy, A. M. Asiri and H. Garcia, *Catal. Sci. Technol.*, 2016, **6**, 5238–5261.
14 S. M. Chavan, G. C. Shearer, S. Svelle, U. Olsbye, F. Bonino, J. Ethiraj, K. P. Lillerud and S. Bordiga, *Inorg. Chem.*, 2014, **53**, 9509–9515.
15 M. Du, C.-P. Li, C.-S. Liu and S.-M. Fang, *Coord. Chem. Rev.*, 2013, **257**, 1282–1305.
16 M. Kim, J. F. Cahill, K. A. Prather and S. M. Cohen, *Chem. Commun.*, 2011, **47**, 7629–7631.
17 S. Marx, W. Kleist, J. Huang, M. Maciejewski and A. Baiker, *Dalton Trans.*, 2010, **39**, 3795–3798.
18 T. Lescouet, E. Kockrick, G. Bergeret, M. Pera-Titus and D. Farrusseng, *Dalton Trans.*, 2011, **40**, 11359–11361.
19 M. Pera-Titus, T. Lescouet, S. Aguado and D. Farrusseng, *J. Phys. Chem. C*, 2012, **116**, 9507–9516.
20 G. Akiyama, R. Matsuda, H. Sato, M. Takata and S. Kitagawa, *Adv. Mater.*, 2011, **23**, 3294–3297.
21 W. J. Phang, H. Jo, W. R. Lee, J. H. Song, K. Yoo, B. Kim and C. S. Hong, *Angew. Chem., Int. Ed.*, 2015, **54**, 5142–5146.
22 W. Lu, D. Yuan, J. Sculley, D. Zhao, R. Krishna and H.-C. Zhou, *J. Am. Chem. Soc.*, 2011, **133**, 18126–18129.
23 N. Reimer, B. Bueken, S. Leubner, C. Seidler, M. Wark, D. De Vos and N. Stock, *Chem. – Eur. J.*, 2015, **21**, 12517–12524.
24 M. Lin Foo, S. Horike, T. Fukushima, Y. Hijikata, Y. Kubota, M. Takata and S. Kitagawa, *Dalton Trans.*, 2012, **41**, 13791–13794.
25 J. Jiang and O. M. Yaghi, *Chem. Rev.*, 2015, **115**, 6966–6997.
26 Y.-H. Liu, Q.-S. Liu and Z.-H. Zhang, *J. Mol. Catal. A: Chem.*, 2008, **296**, 42–46.
27 D. Jiang, T. Mallat, F. Krumeich and A. Baiker, *J. Catal.*, 2008, **257**, 390–395.
28 J. F. Blandez, A. Santiago-Portillo, S. Navalón, M. Giménez-Marqués, M. Álvaro, P. Horcajada and H. García, *J. Mol. Catal. A: Chem.*, 2016, **425**, 332–339.
29 A. Dhakshinamoorthy, M. Alvaro and H. Garcia, *Chem. – Eur. J.*, 2010, **16**, 8530–8536.
30 Y.-X. Zhou, Y.-Z. Chen, Y. Hu, G. Huang, S.-H. Yu and H.-L. Jiang, *Chem. – Eur. J.*, 2014, **20**, 14976–14980.
31 Y. Liu, R. C. Klet, J. T. Hupp and O. Farha, *Chem. Commun.*, 2016, **52**, 7806–7809.
32 Q. Y. Liu, W. F. Wang, Y. L. Wang, Z. M. Shan, M. S. Wang and J. Tang, *Inorg. Chem.*, 2012, **51**, 2381–2392.
33 G. Pawley, *J. Appl. Crystallogr.*, 1981, **14**, 357–361.
34 G. Kresse and J. Hafner, *Phys. Rev. B: Condens. Matter*, 1994, **49**, 14251–14269.
35 K. Lejaeghere, G. Bihlmayer, T. Björkman, P. Blaha, S. Blügel, V. Blum, D. Caliste, I. E. Castelli, S. J. Clark, A. Dal Corso, S. de Gironcoli, T. Deutsch, J. K. Dewhurst, I. Di Marco, C. Draxl, M. Dułak, O. Eriksson, J. A. Flores-Livas, K. F. Garrity, L. Genovese, P. Giannozzi, M. Giantomassi, S. Goedecker, X. Gonze, O. Grånäs, E. K. U. Gross, A. Gulans, F. Gygi, D. R. Hamann, P. J. Hasnip, N. A. W. Holzwarth, D. Iuşan, D. B. Jochym, F. Jollet, D. Jones, G. Kresse, K. Koepernik, E. Küçükbenli, Y. O. Kvashnin, I. L. M. Locht, S. Lubeck, M. Marsman,

 This journal is © The Royal Society of Chemistry 2017

Published on 13 October 2017. Downloaded by Freie Universitaet Berlin on 13/10/2017 09:25:05.

N. Marzari, U. Nitzsche, L. Nordström, T. Ozaki, L. Paulatto, C. J. Pickard, W. Poelmans, M. I. J. Probert, K. Refson, M. Richter, G.-M. Rignanese, S. Saha, M. Scheffler, M. Schlipf, K. Schwarz, S. Sharma, F. Tavazza, P. Thunström, A. Tkatchenko, M. Torrent, D. Vanderbilt, M. J. van Setten, V. Van Speybroeck, J. M. Wills, J. R. Yates, G.-X. Zhang and S. Cottenier, *Science*, 2016, **351**, aad3000.

36 J. P. Perdew, K. Burke and M. Ernzerhof, *Phys. Rev. Lett.*, 1996, **77**, 3865–3868.

37 S. Grimme, J. Antony, S. Ehrlich and H. Krieg, *J. Chem. Phys.*, 2010, **132**, 154104.

38 S. Grimme, S. Ehrlich and L. Goerigk, *J. Comput. Chem.*, 2011, **32**, 1456–1465.

39 D. E. P. Vanpoucke, K. Lejaeghere, V. Van Speybroeck, M. Waroquier and A. Ghysels, *J. Phys. Chem. C*, 2015, **119**, 23752–23766.

40 T. F. Willems, C. H. Rycroft, M. Kazi, J. C. Meza and M. Haranczyk, *Microporous Mesoporous Mater.*, 2012, **149**, 134–141.

41 C. Lee, W. Yang and R. G. Parr, *Phys. Rev. B: Condens. Matter*, 1988, **37**, 785–789.

42 A. D. Becke, *J. Chem. Phys.*, 1993, **98**, 5648–5652.

43 R. Krishnan, J. S. Binkley, R. Seeger and J. A. Pople, *J. Chem. Phys.*, 1980, **72**, 650–654.

44 J. Tomasi, B. Mennucci and R. Cammi, *Chem. Rev.*, 2005, **105**, 2999–3094.

45 I. Senkovska, F. Hoffmann, M. Fröba, J. Getzschmann, W. Böhlmann and S. Kaskel, *Microporous Mesoporous Mater.*, 2009, **122**, 93–98.

46 J. Juan-Alcaniz, R. Gielisse, A. B. Lago, E. V. Ramos-Fernandez, P. Serra-Crespo, T. Devic, N. Guillou, C. Serre, F. Kapteijn and J. Gascon, *Catal. Sci. Technol.*, 2013, **3**, 2311–2318.

47 M. G. Goesten, J. Juan-Alcañiz, E. V. Ramos-Fernandez, K. B. Sai Sankar Gupta, E. Stavitski, H. van Bekkum, J. Gascon and F. Kapteijn, *J. Catal.*, 2011, **281**, 177–187.

48 W. Kleist, M. Maciejewski and A. Baiker, *Thermochim. Acta*, 2010, **499**, 71–78.

49 S. Himeno, T. Komatsu and S. Fujita, *J. Chem. Eng. Data*, 2005, **50**, 369–376.

50 L. H. Wee, M. R. Lohe, N. Janssens, S. Kaskel and J. A. Martens, *J. Mater. Chem.*, 2012, **22**, 13742–13746.

51 B. Yuan, X.-Q. Yin, X.-Q. Liu, X.-Y. Li and L.-B. Sun, *ACS Appl. Mater. Interfaces*, 2016, **8**, 16457–16464.

52 L. H. Wee, F. Bonino, C. Lamberti, S. Bordiga and J. A. Martens, *Green Chem.*, 2014, **16**, 1351–1357.

53 Z. Hu, Y. Peng, K. M. Tan and D. Zhao, *CrystEngComm*, 2015, **17**, 7124–7129.